

Thermal and chemical freeze-out in spectator fragmentation

W. Trautmann,¹ R. Bassini,² M. Begemann-Blaich,¹ A. Ferrero,² S. Fritz,¹ S.J. Gaff-Ejakov,³ C. Groß,¹ G. Immé,⁴ I. Iori,² U. Kleinevoß,¹ G.J. Kunde,^{3,8} W.D. Kunze,¹ A. Le Fèvre,¹ V. Lindenstruth,^{1,9} J. Lukasik,^{1,10} U. Lynen,¹ V. Maddalena,⁴ M. Mahi,¹ T. Möhlenkamp,⁵ A. Moroni,² W.F.J. Müller,¹ C. Nociforo,⁴ B. Ocker,⁶ T. Odeh,¹ H. Orth,¹ F. Petruzzelli,² J. Pochodzalla,^{1,11} G. Raciti,⁴ G. Riccobene,⁴ F.P. Romano,⁴ Th. Rubehn,¹ A. Saija,⁴ H. Sann,^{1,*} M. Schnittker,¹ A. Schüttauf,^{1,6} C. Schwarz,¹ W. Seidel,⁵ V. Serfling,⁶ C. Sfienti,¹ A. Trzciński,⁷ A. Tucholski,⁷ G. Verde,⁴ A. Wörner,¹ Hongfei Xi,¹ and B. Zwiegliński⁷

(The ALADIN Collaboration)

¹*Gesellschaft für Schwerionenforschung mbH, D-64291 Darmstadt, Germany*

²*Istituto di Scienze Fisiche, Università degli Studi di Milano and I.N.F.N., I-20133 Milano, Italy*

³*Department of Physics and Astronomy and National Superconducting Cyclotron Laboratory, Michigan State University, East Lansing, MI 48824, USA*

⁴*Dipartimento di Fisica dell'Università and I.N.F.N., I-95129 Catania, Italy*

⁵*Forschungszentrum Rossendorf, D-01314 Dresden, Germany*

⁶*Institut für Kernphysik, Universität Frankfurt, D-60486 Frankfurt, Germany*

⁷*Soltan Institute for Nuclear Studies, 00-681 Warsaw, Hoza 69, Poland*

⁸*Subatomic Physics Group, Los Alamos National Laboratory, Los Alamos, NM 87545, USA*

⁹*Kirchhoff-Institut für Physik, Universität Heidelberg, D-69120 Heidelberg, Germany*

¹⁰*H. Niewodniczański Institute of Nuclear Physics, PL-31342 Kraków, Poland*

¹¹*Institut für Kernphysik, Universität Mainz, D-55099 Mainz, Germany*

(Dated: October 26, 2018)

Isotope temperatures from double ratios of hydrogen, helium, lithium, beryllium, and carbon isotopic yields, and excited-state temperatures from yield ratios of particle-unstable resonances in ⁴He, ⁵Li, and ⁸Be, were determined for spectator fragmentation, following collisions of ¹⁹⁷Au with targets ranging from C to Au at incident energies of 600 and 1000 MeV per nucleon. A deviation of the isotopic from the excited-state temperatures is observed which coincides with the transition from residue formation to multi-fragment production, suggesting a chemical freeze-out prior to thermal freeze-out in bulk disintegrations.

PACS numbers: 25.70.Mn, 25.70.Pq, 25.75.-q

I. INTRODUCTION

In a disintegration scenario, the products drop out of equilibrium roughly when their interaction rate falls below the expansion rate. A thermal freeze-out is commonly defined as occurring when scattering processes cease to be effective in redistributing the particle momenta. From that time on, apart from sequential decays, only the long-range Coulomb forces continue to modify the otherwise frozen momenta of the disintegration products. Observables depending on the relative momenta, such as two-particle correlation functions, are sensitive to the source properties at the thermal freeze-out time [1, 2]. The relative population of two-particle resonances, in an equilibrium situation, will therefore reflect the temperature at that stage [3, 4].

Chemical freeze-out, on the other hand, is reached once the partitioning into particles and fragments is completed, and mutual scatterings are no longer sufficiently energetic to significantly modify the channel composition by transfer, breakup or capture-type processes. The statistical multifragmentation models assume global equilib-

rium and thus coinciding thermal and chemical freeze-out times [5, 6, 7]. The question to what extent this is found to be realized in nuclear fragmentation reactions has been addressed by several groups. For example, by explicitly taking into account the effects of sequential decay, Huang et al. were able to demonstrate that in central ¹⁹⁷Au on ¹⁹⁷Au collisions at 35 MeV per nucleon the temperatures of the thermal and chemical freeze-out stages are ≈ 4.3 MeV and identical to within 200 keV [8]. A similar observation had earlier been made for ³⁶Ar on ¹⁹⁷Au at the same energy per nucleon [9].

In the central ¹⁹⁷Au on ¹⁹⁷Au reactions, however, when the bombarding energy is increased, temperatures derived from the population of two-particle resonances and from double ratios of isotopic yields start to diverge significantly [10]. The excited-state temperatures saturate at values near $T = 5$ MeV while the isotope temperatures increase to more than 10 MeV at 200 MeV per nucleon, the latter behavior being more in line with what is expected from the increasing system excitation. Differences of similar magnitude have also been reported for ⁸⁶Kr on ⁹³Nb reactions, studied at incident energies up to 120 MeV per nucleon [11]. Calculations showed that sequential decay should alter the two types of temperatures in a coherent fashion and, therefore, cannot account for the observed effect [12].

*deceased

The divergence of isotope and excited-state temperatures in central ^{197}Au on ^{197}Au collisions develops at bombarding energies at which collective radial flow becomes a significant part of the kinetic energies of light particles and fragments [13, 14, 15, 16]. This coincidence was interpreted as indicating a connection with the loss of global equilibrium resulting from the collective expansion. Radial expansion is accompanied by a local cooling which favors cluster formation by coalescence [17], as also demonstrated with nuclear molecular dynamics calculations [18], a process terminated by the rapid rarefaction of the outstreaming material. In this non-equilibrium scenario, the higher temperatures of earlier reaction stages may thus manifest themselves not only in the higher kinetic energies of the fragments but also in partitions representing higher chemical temperatures.

It will be shown in this work that a saturation of excited-state temperatures, while the isotope temperatures rise to higher values, is also observed in spectator fragmentations in which flow effects are less prominent [19, 20, 21, 22, 23]. The divergence starts when the residue formation prevailing at lower excitation energies gives way to the multiple production of intermediate-mass fragments as more energy is deposited in the spectator system. This suggests that it is the more general condition of a bulk breakup, independent of the magnitude of the collective motion accompanying it, which leads to a separation between the chemical and thermal freeze-outs.

Apart from this main conclusion, the paper is also meant to provide a summary of different temperature measurements performed for spectator decays, here specifically for collisions of ^{197}Au nuclei at incident energies of 600 and 1000 MeV per nucleon. Some of the results are already published [10, 21, 24, 25]. Questions addressed in the following, but not necessarily discussed exhaustively, include the Z_{bound} -scaling of spectator decays, the validity of the chemical freeze-out picture, the reliability of sequential-decay corrections, and the magnitude of the internal fragment excitation.

II. EXPERIMENTS AND ANALYSIS

The temperature measurements reported here were performed in two experiments devoted to spectator decays following collisions of ^{197}Au projectiles with a variety of targets ranging from C to Au at bombarding energies of 600 and 1000 MeV per nucleon. In the first experiment, the ALADIN spectrometer was used to detect and identify the products of the projectile-spectator decay [24, 26]. The masses of light fragments were determined by measuring their charge, magnetic-rigidity and velocity. In the second experiment which concentrated on the ^{197}Au on ^{197}Au system at 1000 MeV per nucleon, the target-spectator decay was studied at backward angles with two multi-detector hodoscopes covering the angular range $122^\circ \leq \theta_{\text{lab}} \leq 156^\circ$ and with three high-resolution

telescopes placed at $\theta_{\text{lab}} = 110^\circ, 130^\circ$, and 150° . These detectors were used to measure the yields and correlations of isotopically resolved light charged particles and fragments. The hodoscopes consisted of a total of 160 Si-CsI(Tl) telescopes in closely-packed geometry while the telescopes each consisted of three Si detectors with thickness 50, 300, and 1000 μm and of a 4-cm long CsI(Tl) scintillator with photodiode readout. Further details and results obtained in the second experiment may be found in Refs. [10, 21, 25, 27].

In both experiments, the variable Z_{bound} , as measured for the projectile spectator with the ALADIN time-of-flight wall, was used for sorting the data according to impact parameter. Z_{bound} is defined as the sum of the atomic numbers Z_i of all projectile fragments with $Z_i \geq 2$. It reflects the variation of the charge of the primary spectator system and is monotonically correlated with the impact parameter of the reaction [28]. In the second experiment, when the decay of the target spectator was studied, the impact-parameter selection with the Z_{bound} of the projectile took advantage of the symmetry of the ^{197}Au on ^{197}Au system [25].

The excited-state temperatures are deduced from the populations of particle-unstable resonances in emitted ^4He , ^5Li and ^8Be nuclei, determined from two-particle coincidences measured with the Si-CsI hodoscopes. The peak structures were identified by using the technique of correlation functions, and background corrections were based on results obtained for resonance-free pairs of light fragments. The pair of the ground state (g.s.) and 16.66-MeV excited state of ^5Li , identified in p- ^4He and d- ^3He coincidence yields, represents a widely used thermometer for nuclear reactions [3, 29, 30]. In addition, correlated yields of p-t, p- ^7Li , and ^4He - ^4He coincidences and ^4He single yields were used to deduce temperatures from the relative populations of states or groups of states in ^4He (g.s.; 21.21 MeV and higher) and in ^8Be (3.04 MeV; 17.64 and 18.15 MeV). The relative efficiencies for the correlated detection of the decay products were calculated with a Monte Carlo model [29, 31, 32]. The estimated uncertainties of the background functions are the main contributions to the errors of these excited-state temperatures.

The isotope temperatures were deduced from the double ratios of yields of neighboring isotopes, as described previously [24, 25, 33]. Energy-integrated yields were measured for the projectile decay for which the acceptance of the ALADIN spectrometer provides good solid-angle coverage. For the target spectator, isotopically resolved yields were obtained from the four-element telescopes. Besides the commonly used T_{HeLi} thermometer, based on the $^3\text{He}/^4\text{He}$ and $^6\text{Li}/^7\text{Li}$ yield ratios, temperature observables deduced from other pairs of isotopes were also evaluated. The corresponding expressions are

$$T_{\text{HeLi}} = 13.3 \text{ MeV} / \ln(2.2 \frac{Y_{^6\text{Li}}/Y_{^7\text{Li}}}{Y_{^3\text{He}}/Y_{^4\text{He}}}). \quad (1)$$

$$T_{\text{HePd}} = 18.4 \text{ MeV} / \ln(5.5 \frac{Y_p/Y_d}{Y_{3\text{He}}/Y_{4\text{He}}}). \quad (2)$$

$$T_{\text{HeDt}} = 14.3 \text{ MeV} / \ln(1.6 \frac{Y_d/Y_t}{Y_{3\text{He}}/Y_{4\text{He}}}). \quad (3)$$

$$T_{\text{BeLi}} = 11.3 \text{ MeV} / \ln(1.8 \frac{Y_{9\text{Be}}/Y_{8\text{Li}}}{Y_{7\text{Be}}/Y_{6\text{Li}}}). \quad (4)$$

$$T_{\text{tHeLiBe}} = 14.2 \text{ MeV} / \ln(2.2 \frac{Y_{6\text{Li}}/Y_{7\text{Be}}}{Y_t/Y_{4\text{He}}}). \quad (5)$$

$$T_{\text{CLi}} = 11.5 \text{ MeV} / \ln(5.9 \frac{Y_{6\text{Li}}/Y_{7\text{Li}}}{Y_{11\text{C}}/Y_{12\text{C}}}). \quad (6)$$

$$T_{\text{CC}} = 13.8 \text{ MeV} / \ln(7.9 \frac{Y_{12\text{C}}/Y_{13\text{C}}}{Y_{11\text{C}}/Y_{12\text{C}}}). \quad (7)$$

The prefactors in Eqs. (1)-(7) represent the double differences of the binding energies of the four isotopes appearing in the double yield ratios. They are between 11 and 19 MeV and thus fulfill the requirement that this quantity should be large compared to the anticipated temperatures [34, 35]. The numerical factors preceding the double yield ratios in the denominator contain the mass numbers and the ground-state degeneracies $2s_{\text{g.s.}} + 1$ of these isotopes [34]. The expressions are thus strictly valid only for the ground-state populations in thermal equilibrium. Since they may be subsequently altered by the feeding from excited states and from particle-unbound resonances, temperatures obtained with these expressions from measured yields are referred to as apparent temperatures. The magnitude of the corrections required to account for these effects was estimated on the basis of calculations with the Quantum Statistical Model of Hahn and Stöcker [36] in the version of Konopka et al. [37], but also with other statistical models as described previously [24, 25] and discussed below.

III. RESULTS

Temperature values obtained for ^{197}Au on ^{197}Au at 1000 MeV per nucleon are summarized in Fig. 1, top, where they are displayed as a function of Z_{bound} . The closed symbols represent the isotope temperature T_{HeLi} as derived for the target spectator from the energy-integrated yields measured at $\theta_{\text{lab}} = 150^\circ$ and for the projectile spectator from the measured total yields. They include a correction factor 1.2 to account for the effects of secondary decays which was obtained as an average over the predictions of several statistical models [24, 25]. The

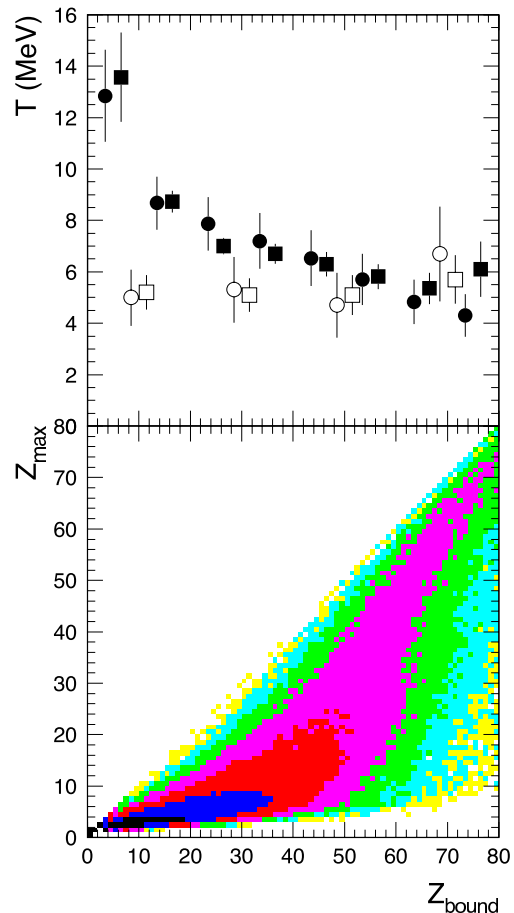


FIG. 1: (Color online) Results obtained for ^{197}Au on ^{197}Au at $E/A = 1000$ MeV: Top: Measured isotope temperature T_{HeLi} (full circles and squares representing the data for the target and projectile decays, respectively) and excited-state temperatures (open circles and squares representing the data for ^5Li and ^4He , respectively) as a function of Z_{bound} . Average values for 10 or 20 unit intervals of Z_{bound} are given. For clarity, the data symbols are slightly displaced horizontally. The indicated uncertainties are mainly of systematic origin. Bottom: Distribution of Z_{max} versus Z_{bound} after conventional fission events have been removed. The shadings follow a logarithmic scale.

two data sets agree within errors as expected because of the symmetry of the reaction. The different solid-angle coverage and detection techniques, apparently, do not cause measurable differences.

The open symbols represent the temperatures deduced from the ratios of state populations in ^4He and ^5Li , integrated over 20-unit intervals of Z_{bound} for reasons of counting statistics. In striking contrast to the isotope temperature T_{HeLi} which monotonically rises up to about 12 MeV, they are virtually independent of Z_{bound} , mutually consistent with each other, and define a mean value of ≈ 5 MeV. A temperature $T_{\text{sBe}} = 5.6 \pm 1.2$ MeV, averaged over the full range of Z_{bound} because of low count rates, was derived from the ratio of excited-state populations in ^8Be . A similar behavior was observed for central

^{197}Au on ^{197}Au collisions when the energy was raised from 50 up to 200 MeV per nucleon [10].

An important characteristic of the spectator decay is illustrated in Fig. 1, bottom. It shows the event distribution in the Z_{max} -versus- Z_{bound} plane, where Z_{max} denotes the largest atomic number Z observed in the event. At large Z_{bound} , corresponding to small excitation energies, Z_{max} is very close to Z_{bound} , indicating that mainly one large fragment or heavy residue is produced. At small Z_{bound} and high excitations, Z_{max} is much smaller than Z_{bound} which implies that the disintegration has additionally produced several other fragments, as equally evident from the measured multiplicity distributions [26]. The transition between these two regimes, at Z_{bound} between 50 and 60, is marked by a fairly rapid drop of the ridge line representing the most probable Z_{max} .

Using a simplified statistical model for multifragmentation, Das Gupta and Mekjian have shown that the decrease of the relative mass of the largest fragment with respect to the system mass, A_{max}/A_0 , is rather sharp if regarded on the temperature scale [38]. At this temperature, termed "boiling temperature" by the authors, a peak in the specific heat develops which becomes increasingly pronounced as the system mass A_0 is increased to large values, $A_0 > 1000$, i.e., far beyond the limits of nuclear masses. For $A_0 = 150$, the system mass corresponding to $Z_{\text{bound}} \approx 50$ [24], the predicted specific heat distribution is wider with a maximum at $T = 6.3$ MeV. This is slightly larger than the value $T_{\text{HeLi}} = 5.8 \pm 0.8$ MeV measured for $50 < Z_{\text{bound}} < 60$ but, within errors, consistent with it. In this respect, a link may be seen between the observed onset of multi-fragment disintegrations and the first-order phase transition expected for large nuclear systems. The two temperature observables, incidentally, start to deviate from each other in this transition region.

The invariance of Z_{bound} -sorted fragment multiplicities and related observables describing the partitioning of the system represents a prominent characteristic of spectator fragmentation. The validity of Z_{bound} scaling with respect to the choice of the target was one of the early indications for equilibrium being reached at breakup [39, 40]. This invariance property is also shared by the chemical freeze-out temperature T_{HeLi} as shown in Fig. 2, bottom, for the projectile decay at 600 MeV per nucleon after collisions with target nuclei ranging from carbon to gold. The mass of the target only determines which part of the Z_{bound} range will be populated in the reaction (Fig. 2, top). Heavy targets are required for initiating the most violent collisions associated with small Z_{bound} .

The thermometry with the $^{3,4}\text{He}$ isotope pairs benefits from the large difference $\Delta B = 20.6$ MeV of the binding energies of these two nuclei but it is not the only choice. There are also other combinations of isotopes which can be expected to provide the necessary sensitivity for the measurement of temperatures in the MeV range. The additional cases studied here are the thermometers T_{BeLi} , T_{HeLiBe} , T_{CLi} , and T_{CC} (Eqs. (4)-(7)). In T_{HeLiBe} , ^3He

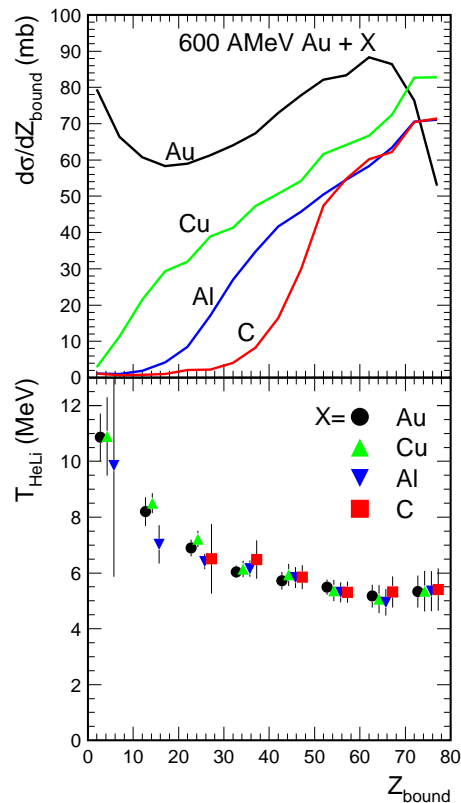


FIG. 2: (Color online) Top: Measured cross sections $d\sigma/dZ_{\text{bound}}$ for the reactions of ^{197}Au projectiles at $E/A = 600$ MeV with targets of C, Al, Cu, and Au. Note that the experimental trigger affected the cross sections for $Z_{\text{bound}} \geq 65$. Bottom: Isotope temperature T_{HeLi} measured for the same four reactions presented as averages over 10-unit wide bins of Z_{bound} . For clarity, the data symbols are slightly displaced horizontally.

is replaced by the triton which has a very similar binding energy, and consequently also ^7Li by ^7Be . The T_{BeLi} thermometer is interesting because it is exclusively based on fragments with $Z \geq 3$ and not on light-particle yields. With the carbon thermometers T_{CLi} and T_{CC} one hopes to exploit the large difference of the $^{11,12}\text{C}$ binding energies of $\Delta B = 18.7$ MeV. Their use can permit a test of chemical equilibrium up to this range of fragment masses.

Measured isotope ratios, as needed for these thermometers, are shown in Fig. 3. For the $^{3,4}\text{He}$ and $^{6,7}\text{Li}$ isotope pairs, ratios obtained for the integrated yields of projectile fragments at 600 MeV per nucleon and for the yields of target fragments measured at $\theta_{\text{lab}} = 150^\circ$ and 1000 MeV per nucleon agree within errors. Since this is again a manifestation of Z_{bound} scaling, here of the invariance with bombarding energy [25, 26], the distinction between these cases will be dropped in the following. Of the eight yield ratios shown, only the $^{3,4}\text{He}$ ratio and, less

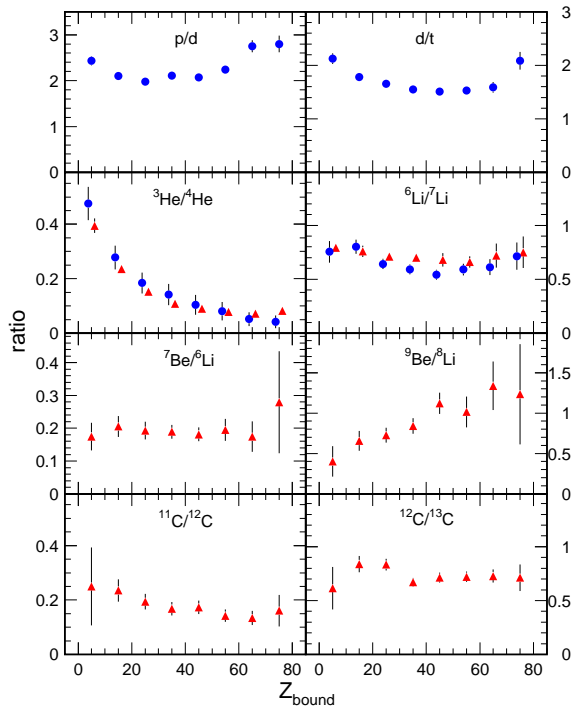


FIG. 3: (Color online) Measured isotope yield ratios for ^{197}Au on ^{197}Au reactions as a function of Z_{bound} . Results obtained for projectile fragments at 600 MeV per nucleon and for target fragments at 1000 MeV per nucleon incident energy are represented by triangles and circles, respectively.

pronounced, also the $^9\text{Be}/^8\text{Li}$ ratio ($\Delta B = 16.9$ MeV) vary strongly with Z_{bound} . For $^{11,12}\text{C}$, the total variation amounts to hardly a factor of 2, less than the factor 3 for $^9\text{Be}/^8\text{Li}$, while the other ratios are rather flat. For these remaining five pairs of isotopes, this is not unexpected because the differences of their binding energies are within $\Delta B = 2.2$ MeV (p,d) and $\Delta B = 7.3$ MeV ($^{6,7}\text{Li}$).

Results for six temperatures obtained with these ratios are shown in Fig. 4. They have been corrected for the effect of secondary decays by using the predictions of the quantum statistical model [36, 37], calculated for a breakup density $\rho/\rho_0 = 0.3$. With the exception of T_{CLi} , all temperatures increase slowly as the collisions pass through the rise and fall of fragment production with decreasing Z_{bound} . The values are about 4 to 6 MeV for peripheral collisions and reach 8 to 10 MeV for the most violent fragmentations at small impact parameters. The rise is, notably, also observed with T_{BeLi} and thus not a singular consequence of the behavior of the $^{3,4}\text{He}$ yield ratio. Only the carbon-lithium thermometer does not fit into this otherwise rather consistent picture. Here the small variations of the $^{11,12}\text{C}$ and $^{6,7}\text{Li}$ yield ratios, apparently, compensate each other (Fig. 3), leading to a nearly constant temperature which is not changed much by the corrections. At very large and very small Z_{bound} , at the boundaries of the fragmentation regime, the errors

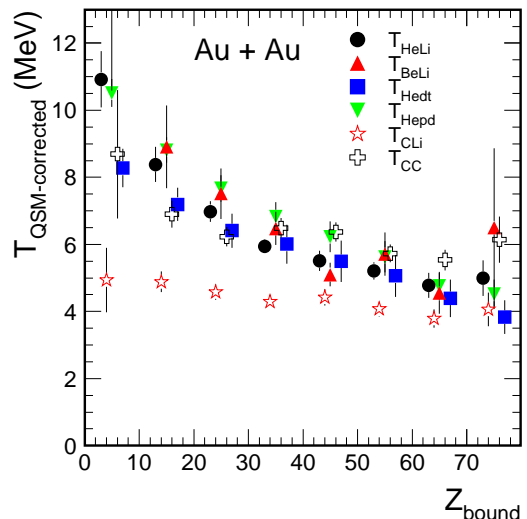


FIG. 4: (Color online) Isotope temperatures for ^{197}Au on ^{197}Au at 600 and 1000 MeV per nucleon, with corrections for the effects of secondary decay according to the quantum statistical model [36, 37], as a function of Z_{bound} .

are large for temperatures deduced from beryllium and carbon isotopes because the yields are small.

IV. DISCUSSION

A. Target invariance

Reports of a saturation of the breakup temperature at high excitation energies in ^{197}Au on ^{12}C at 1000 MeV per nucleon [41] and of a difference between this and the ^{197}Au on ^{197}Au reactions have led to discussions in the literature [42] and have inspired theoretical investigations into their possible origin [43]. In the present data, no significant difference is observed for reactions of the ^{197}Au projectiles with different targets if the temperature is viewed as a function of Z_{bound} (Fig. 2). As the Z_{bound} region populated with the lighter targets is limited, comparisons will have to be restricted to the common range. In the data of the EOS collaboration [41, 44], with ^{197}Au on ^{12}C covering the rise of fragment production, the temperature T_{HeDt} , e.g., rises from about 4 to 6 MeV with increasing centrality. This is very similar to the results obtained here for $Z_{\text{bound}} > 40$, the corresponding interval in ^{197}Au on ^{197}Au (Fig. 4). The corrections are small for T_{HeDt} (see below) which permits a direct comparison of the two data sets.

In the present studies of projectile fragmentation, the apparent tails of the cross section $d\sigma/dZ_{\text{bound}}$ toward smaller values of Z_{bound} (Fig. 2, top) can be quantitatively assigned to background reactions in thin plastic detectors mounted about 1.5 m upstream of the target. These detectors containing scintillator material with a total areal density of typically 15 mg/cm² were used to

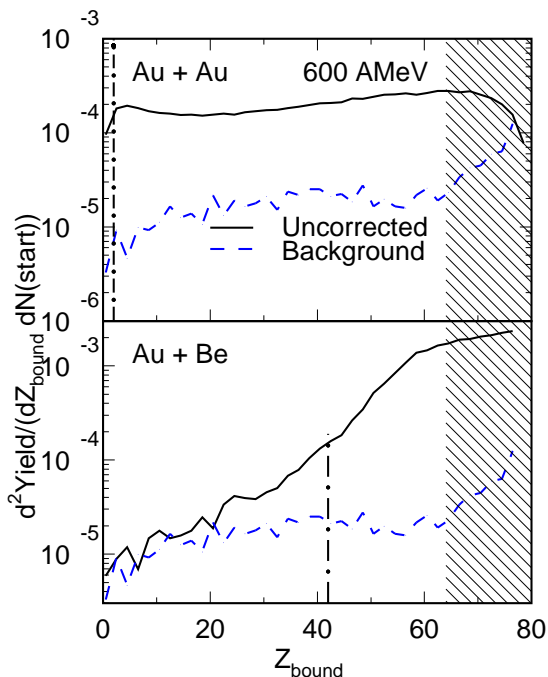


FIG. 5: Cross sections $d\sigma/dZ_{\text{bound}}$ (in units of events per projectile) for the reactions of ^{197}Au projectiles at $E/A = 600$ MeV with the two targets of Au (top) and Be (bottom) before background subtraction (full line) and background generated by upstream detectors (dashed). The dash-dotted lines indicate the value of Z_{bound} at which the cross-section integral has reached a relative value of 1.5%. Inefficiencies of the experimental trigger affect the range $Z_{\text{bound}} \geq 65$ (hatched).

measure the arrival time and transverse coordinates of the incoming beam particles. The ALADIN spectrometer has an increasingly reduced acceptance for reactions occurring further upstream. In reactions occurring there, some of the produced projectile fragments may, therefore, escape detection, and the recorded Z_{bound} will be too small. The yield of reactions in these foils, measured by removing the regular target, is shown in Fig. 5 in comparison with the cross sections $d\sigma/dZ_{\text{bound}}$ measured for reactions of the ^{197}Au projectiles with the regular targets of ^{197}Au (480 mg/cm^2) and ^9Be (700 mg/cm^2). The figure demonstrates that the population of the region $Z_{\text{bound}} < 30$, corresponding to excitations of $E/A > 10$ MeV [24], is negligible if a beryllium target is used. The tail of the cross section at $Z_{\text{bound}} < 45$ ($E/A > 8$ MeV) is on the percent level and may even be partly due to fluctuations caused by other small experimental inefficiencies and by secondary reactions within the target and detectors. In the analysis of the present experiments, the first 1.5% of the integrated reaction cross section at small Z_{bound} in the corrected spectrum (to the left of the dashed-dotted lines in Fig. 5) have been ignored (see also Ref. [26]).

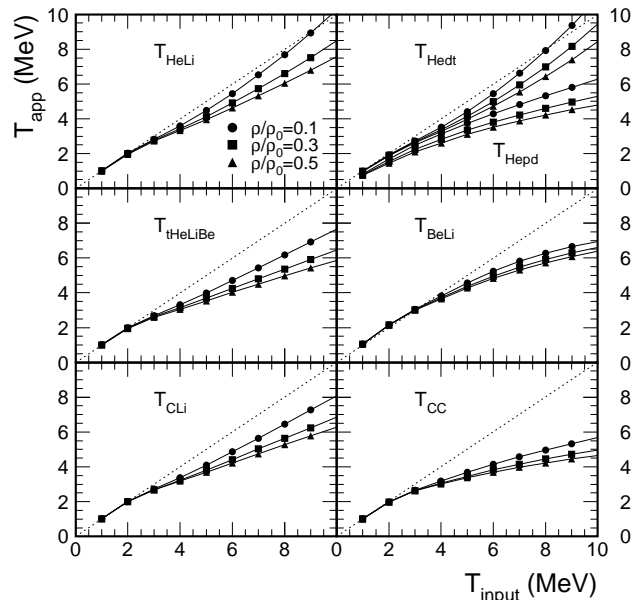


FIG. 6: Apparent temperatures T_{app} as a function of the temperatures T_{input} used in calculations with the quantum-statistical model of Refs. [36, 37] (full lines) for the seven temperature observables of Eqs. (1)-(7). The symbols distinguish three assumptions for the breakup density as indicated in the left top panel. The dotted lines mark the diagonal $T_{\text{app}} = T_{\text{input}}$.

B. Corrections

The need to consider the effects of secondary decay is known since breakup temperatures are being measured and was respected in the study of ^{197}Au fragmentations [24]. Besides the ground states considered in Eqs. (1)-(7) also excited states are expected to be populated according to the equilibrium conditions and both may be fed by particle decays of heavier products. The problem has been addressed by several groups and, besides the work already cited (Refs. [3, 8, 9, 11, 12, 25, 35, 42]), the reader is referred to Refs. [45, 46, 47, 48, 49] and references cited therein.

In the following, the corrections for the isotope temperatures predicted by the quantum-statistical model of Hahn and Stöcker [36, 37] will be discussed in more detail. This model assumes thermal and chemical equilibrium at breakup at which the fragmenting system is characterized by a density ρ , temperature T , and by its overall N/Z ratio. Fermion and boson statistics are respected which, however, is not crucial at high temperature. The model does not consider the finite size of nuclear systems but follows the sequential decay of excited fragments according to tabulated branching ratios. It is exact in this respect, within the limits of its associated mass table.

Results obtained with this model for the seven temperature observables given in Eqs. (1)-(7) are shown in Fig. 6. The apparent temperatures T_{app} , as deduced from

the formulas, are shown as a function of the equilibrium temperatures T_{input} of the fragmenting system for which breakup densities between $\rho = 0.1 \rho_0$ and $\rho = 0.5 \rho_0$ were assumed. At low temperatures, the population of higher states is less important, and T_{app} is very close to T_{input} as expected. The deviations at higher temperatures $T > 3$ MeV are smallest for the two observables T_{HeLi} and T_{Hedt} but not negligible. For T_{HeLi} at $T_{\text{input}} = 6$ MeV, the apparent T_{HeLi} is between 4.5 and 5.5 MeV, depending on the density. The deviations are generally larger for the higher densities. For T_{HeLi} and $\rho = 0.3 \rho_0$, the predicted correction is well described by $T_{\text{input}} = 1.2 \cdot T_{\text{app}}$, suggesting a global correction factor 1.2. A similar value has been derived as an average from calculations with several statistical models [24], including GEMINI [50] and the Berlin microcanonical multifragmentation model MMMC [5]. It was used for T_{HeLi} in previous work (Refs. [10, 21, 24, 25, 51]) and applied also here to obtain the results shown in Figs. 1 and 2. A correction of 20% is indicated also by calculations with the Copenhagen Statistical Fragmentation Model as shown in Ref. [25].

The predicted deviations of T_{app} from T_{input} at higher temperatures are considerably larger for the other observables, notably for T_{Hepd} and T_{CC} ; small differences of T_{app} correspond to large differences of T_{input} which makes these temperatures less precise. This is reflected by the errors adopted for the results shown in Fig. 4 for which the QSM predictions for $\rho = 0.3 \rho_0$ were used for the corrections. Calculations were also performed with the model of Tsang, Xi et al. [35, 47] which is partly adapted to binary emissions and has been found to consistently reproduce observed variations of T_{app} in several reactions, including the ^{197}Au on ^{197}Au reaction at 35 MeV per nucleon cited above [8]. The results are qualitatively similar to those obtained with the QSM except for T_{CLi} and T_{CC} for which much smaller corrections are obtained (for details see [52]). In these cases, the predicted apparent temperatures seem to depend very sensitively on the model assumptions.

The temperature observables associated with the largest predicted uncertainties, T_{Hepd} , T_{CLi} and T_{CC} , are incidentally also those with the largest deviations from the common behavior of the others. Their apparent values depend very little on Z_{bound} and those involving carbon isotope ratios essentially saturate, an observation also made for the central ^{197}Au on ^{197}Au collisions at 50 to 200 MeV per nucleon (Fig. 7, right panel, Ref. [10]). According to the QSM, this behavior is expected for T_{Hepd} and T_{CC} , and the calculated corrections suffice to restore the consistency with the others. This is not the case for T_{CLi} for which only small corrections are predicted. According to the model of Tsang, Xi et al., the corrections should be small for both temperatures based on the $^{11,12}\text{C}$ yield ratio, leading to similar carbon temperatures of approximately 4 MeV, with no significant Z_{bound} dependence. In either case, the concept of a common freeze-out temperature is not supported by

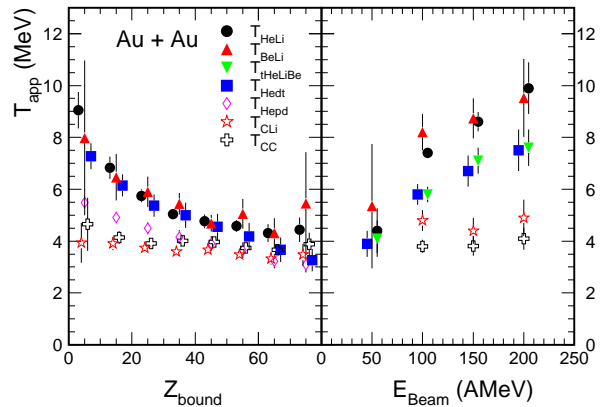


FIG. 7: (Color online) Apparent isotope temperatures (Eqs. (1)-(7)) in ^{197}Au on ^{197}Au reactions for spectator decays at 600 and 1000 MeV per nucleon as a function of Z_{bound} (left panel) and for central collisions at 50 to 200 MeV per nucleon as a function of the incident energy (right panel).

the isotope temperatures deduced from carbon isotope yields.

The three excited-state temperatures are characterized by large energy differences of the considered states, and, as done previously, no corrections for sequential feeding were applied [10, 11]. This is best justified for the case of the particle-unstable resonances of ^5Li [3, 32, 45] and found valid also for ^4He as long as the temperature is low (≈ 4 MeV or less, cf. [8]). However, side-feeding contributions to the measured α particle yields should have similar consequences for both, the excited-state and double-isotope temperatures, as discussed in Ref. [12]. Applying the correction factor of 1.2 used for T_{HeLi} will raise the ^4He temperature to about 6 MeV but will not modify its invariance with respect to Z_{bound} (Fig. 1). Within errors, also the consistency with the ^5Li temperature will be maintained. The ^8Be thermometer requires a side-feeding correction of 1.1 ± 0.1 , according to the calculations [32], which will raise the Z_{bound} -averaged result to 6.2 ± 1.5 MeV.

The observed saturation of the excited-state temperatures has interesting consequences also for the side-feeding corrections of the isotope temperatures. Generally, one would expect that the corrections are less important if the emerging fragments are less excited. The corrections for higher temperatures may, therefore, be overestimated if chemical and thermal equilibrium at breakup is assumed as in the QSM. However, if the chemical freeze-out precedes the thermal freeze-out, as the divergence of the temperatures suggests, the evolution of the system from one to the other will still have to be accounted for. There, the preformed fragments are unlikely to have reached their asymptotic quantum structure, and standard decay probabilities and branching ratios would not necessarily be adequate for that pur-

TABLE I: Corrected double-isotope temperatures T_{HeLi} as obtained with four methods, (a) using the QSM predictions for $\rho = 0.1 \rho_0$ as shown in Fig. 6, (b) using the global correction factor 1.2 which is representative for the QSM results with $\rho = 0.3 \rho_0$, (c) by applying the QSM correction factor for 5 MeV ($0.1 \rho_0$) for $T_{\text{app}} \geq 5$ MeV, and (d) by using the empirical correction factor for 4.3 MeV of Ref. [12]. All values are given in MeV.

T_{app}	$T_{\text{QSM}(0.1\rho_0)}$	$1.2 \cdot T_{\text{app}}$	$T_{\text{QSM}(5 \text{ MeV})}$	$T_{\text{MSU}(4.3 \text{ MeV})}$
5	5.6	6.0	5.7	4.9
6	6.6	7.2	7.0	5.8
7	7.4	8.4	8.5	6.8
8	8.2	9.6	10.0	7.7
9	9.1	10.8	11.6	8.6

pose. In-medium properties of fragments in the hot environment are, in fact, attracting considerable interest presently, with modifications being indicated by isotopic effects observed in recent studies of fragment production (see, e.g., Refs. [51, 53, 54, 55, 56] and references therein).

The order of magnitude of the effects to be expected may perhaps be illustrated by applying correction factors obtained for $T \approx 5$ MeV, the saturation temperature for internal excitations, to chemical temperatures higher than that value. More precisely, in the terminology introduced in Ref. [35], the calculated correction factor κ for the double yield ratio at $T_{\text{app}} = 5$ MeV is used for correcting all $T_{\text{app}} \geq 5$ MeV. With this procedure, the values for, e.g., T_{BeLi} at $Z_{\text{bound}} \approx 15$ and 25 (Fig. 4) will be reduced by 1.2 MeV and 0.6 MeV, respectively. The values for T_{HeLi} will increase, as shown in Table I where they are compared to the other correction methods discussed up to now. For completeness, also the temperatures obtained with the empirical factor κ deduced for central ^{197}Au on ^{197}Au collisions at 35 MeV per nucleon ($T \approx 4.3$ MeV, Ref. [12]) are given in the table (last column). These values are even slightly smaller than T_{app} by up to 5% and should probably be taken as lower limits (the corrected temperature should be larger than T_{app} if the sequential production of ^4He is strong). Altogether, these results may be considered as representative for the increasing systematic uncertainty as the temperature to be measured increases.

C. Kinetic energies

In the kinetic-energy spectra of light products from the ^{197}Au on ^{197}Au reaction, a soft component characterized by temperatures of the order of 5 MeV or lower is well recognized for protons, neutrons, and α particles. For protons and neutrons, this has been shown in [21, 57, 58]. For the case of α particles from the target-spectator decay at 1000 MeV per nucleon, this is illustrated in Fig. 8. Besides the measured spectra, the figure

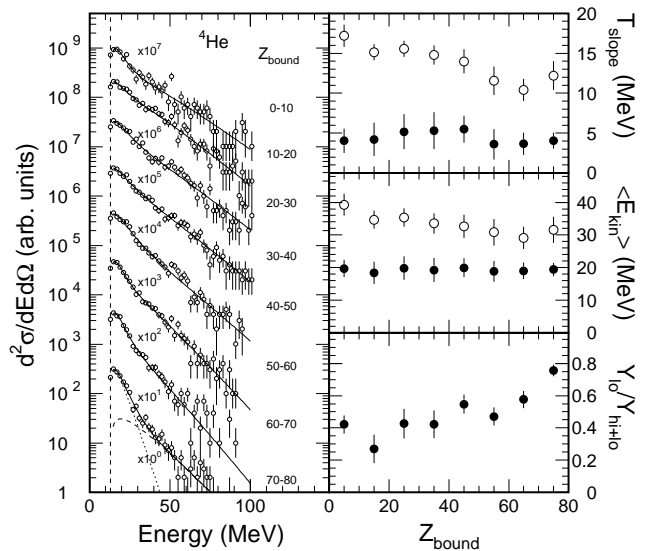


FIG. 8: Energy spectra of ^4He measured at $\theta_{\text{lab}} = 135^\circ$ for the reaction ^{197}Au on ^{197}Au at 1000 MeV per nucleon for eight intervals of Z_{bound} (left panel). The full lines represent the results of a fit with two Maxwellian sources whose individual contributions are shown for the bin of largest Z_{bound} (dotted and dashed lines). The vertical dashed line indicates the threshold for identification. The obtained slope temperatures, mean kinetic energies and relative strengths of the high and low-temperature components are represented by the open and closed circles, respectively (right panels).

shows the slope temperatures, mean kinetic energies and relative intensities obtained from a two-component fit with Maxwellian sources. The low-temperature component dominates for large Z_{bound} but drops to a strength of about 40% for smaller Z_{bound} . Interpreting it as resulting from secondary emissions is consistent with the evolution of the reaction process (Fig. 1). Below the fragmentation threshold (large Z_{bound}), the observed α particle yields are expected to be mainly produced by evaporation from excited heavy residues. In the domain of multifragmentation, secondary emission from heavier fragments should contribute only a fraction of the total yield. The fitted slope temperatures of 4 to 5 MeV are compatible with either process, evaporation as well as secondary emission from nuclei in thermal equilibrium at the break-up temperature.

With the assumption that the identified low-temperature component is the main reason for the need of corrections, He-Li isotope temperatures can be derived using only the high-temperature yields of α particles without further corrections. The results for this new temperature T_{hi} are given in Table II. The effective correction factors $R_{\text{hi}} = T_{\text{hi}}/T_{\text{app}}$ with respect to the apparent temperature, as obtained from the energy-integrated yields according to Eq. (1), are between 1.3 and 1.4 and higher than the corrections for T_{HeLi} used up to now (Table I). Accordingly, the resulting T_{hi} is about 1 MeV

TABLE II: He-Li double-isotope temperature T_{hi} derived by using only the high-temperature fraction y_{hi} of α particles (Fig. 8), without further corrections, for four bins of Z_{bound} . R_{hi} is the corresponding effective correction factor. The errors given for T_{hi} and R_{hi} result from the quoted uncertainty of y_{hi} obtained in the fitting procedure.

Z_{bound}	T_{app} (MeV)	y_{hi}	T_{hi} (MeV)	R_{hi}
0-20	8.0	$0.62 \pm .05$	$11.2 \pm .8$	$1.40 \pm .09$
20-40	5.5	$0.57 \pm .06$	$7.2 \pm .4$	$1.30 \pm .07$
40-60	5.0	$0.49 \pm .04$	$6.8 \pm .3$	$1.37 \pm .06$
60-80	4.5	$0.28 \pm .03$	$7.9 \pm .5$	$1.76 \pm .11$

higher than the temperatures given in Figs. 1,2, and 4. In the bin of largest Z_{bound} , the relative correction is even larger, leading to a T_{hi} similar to the ≈ 7 MeV obtained for the neighboring bins in which multifragmentation represents the main reaction channel. Here, as the inspection of Fig. 1 shows, heavy-residue production dominates but the fluctuations of Z_{max} are already large. For a possible interpretation, T_{hi} may, therefore, be assigned to multifragmentation events which are weak in this bin of Z_{bound} but perhaps exclusively selected by gating on the high-temperature α component.

The systematic errors associated with T_{hi} are enhanced by the difficulty of reliably identifying the evaporation component in the spectra (Fig. 8). The quoted errors $\Delta y_{hi} \approx 0.05$, obtained in the spectra-fitting procedure, correspond to a temperature change of typically $\Delta T_{hi} \approx 0.5$ MeV (Table II). The true uncertainties are likely to be larger even though secondary α components of 40% in multifragmentation seem very reasonable. For example, they compare well with the 26% to 42% determined with correlation techniques for central Xe on Sn collisions at 32 to 50 MeV per nucleon [59].

This alternative and purely experimental method of considering the effects of secondary decays may be seen as providing another estimate for the magnitude of systematic errors but also as globally confirming the obtained chemical breakup temperatures of 6 to 7 MeV for Au fragmentations.

Equilibrium including the kinetic degrees of freedom is, apparently, not achieved in the present reactions. The slope temperatures of 12 to 17 MeV of the high-temperature component, assigned here to multifragmentation events, are considerably higher than the chemical temperatures. They are, furthermore, nearly independent of the fragment mass in the range $A \leq 10$ [21] which rules out collective motions as their origin. A significant collective flow should also become apparent in the impact-parameter dependence of the kinetic energies which is not the case (Fig. 8). Finite flow values have, nevertheless, been reported for spectator reactions but were derived from comparisons with statistical-model calculations (which assume kinetic equilibration) and by assigning a collective origin to measured excess energies

[22, 60, 61]. An alternative explanation has been given by Odeh et al. [21] who have shown that, within the Goldhaber model of a random superposition of nucleon momenta [62], the larger slope temperatures are consistent with a chemical freeze-out at 6 to 8 MeV (see also Refs. [20, 63] for discussions of this scenario).

D. Chemical freeze-out

The rise at small Z_{bound} , i.e. high excitation energy, observed with T_{HeLi} (Figs. 1,2) is well reproduced by most thermometers, including T_{BeLi} which is derived from the ${}^7,9\text{Be}$ and ${}^6,8\text{Li}$ isotope ratios (Fig. 4). There is, overall, good agreement between the different temperature observables with the exception of those containing carbon isotopes. In the latter cases, the apparent temperature values remain approximately constant with values between 4 and 5 MeV (Fig. 7). For T_{CC} (${}^{11,12}\text{C}$ and ${}^{12,13}\text{C}$), a large correction is required according to the QSM calculations (Fig. 6) which lifts T_{CC} into the range of values assumed by the other temperature observables but T_{CLi} remains low. With the corrections according to Tsang, Xi et al. [35, 47], both temperatures involving carbon isotopes will remain near 5 MeV or below. In either case, a freeze-out state in chemical and thermal equilibrium including the carbon and possibly heavier isotopes seems to be excluded with a tendency of heavier fragments having to come from colder regions of the system, as suggested by calculations within the quantum-molecular dynamics model [64, 65].

A slightly different interpretation, based on measurements for a subset of the temperature observables studied here, has been proposed in Ref. [11]. For the central ${}^{86}\text{Kr}$ on ${}^{93}\text{Nb}$ collisions, two isotope thermometers T_{HeLi} and T_{CLi} were compared with the excited-state thermometers ${}^4\text{He}$, ${}^5\text{Li}$, and ${}^8\text{Be}$. Of these only the T_{HeLi} temperature exhibited a rise with the bombarding energy which suggested the conclusion that differences in the production environment of ${}^3\text{He}$ may be responsible for the singular behavior of T_{HeLi} . While this cannot explain the common behavior of T_{BeLi} and T_{HeLi} observed in this work, it also points toward a more general scenario of different freeze-out conditions for different products, possibly also connected with the cooling prior to and during the freeze-out process [66].

In contrast to central collisions of symmetric systems, there is no strong indication of collective radial flow in spectator decays, neither in the mass dependence of the kinetic energies of particles and fragments [21, 25] nor in their absolute magnitude [19], as discussed in the previous subsection. Therefore, if the different behavior of the excited-state and isotope temperatures for light fragments is assumed to have a common cause in both types of reactions, the collective flow by itself is not a very likely candidate for it. A more general common property of the two types of reactions is the disintegration of the whole system into many fragments and particles as the

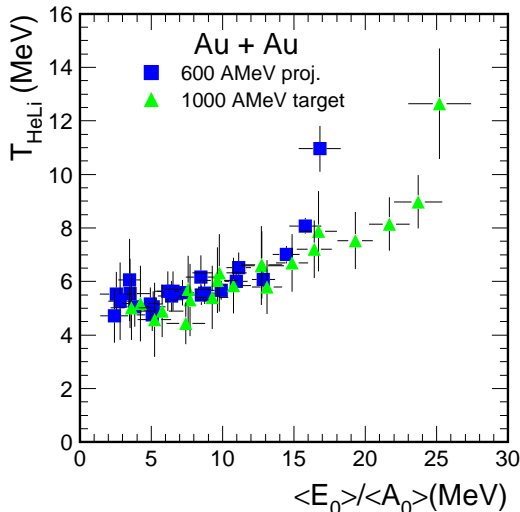


FIG. 9: (Color online) Caloric curves obtained for ^{197}Au on ^{197}Au at 600 and 1000 MeV per nucleon with temperatures T_{HeLi} and excitation energies from calorimetry including the LAND data for neutrons [24, 52].

collisions become more violent. The maximum multiplicities of intermediate-mass fragments, after normalization with respect to the mass of the system, are of similar magnitude in central ^{197}Au on ^{197}Au collisions at 100 MeV per nucleon and in the spectator decays discussed here [19].

A rise of the temperature with decreasing Z_{bound} can be expected because the collisions become more violent. The fragment mass spectra change rapidly and become increasingly steep [40]. Primarily, this indicates an increase in deposited excitation energy [67, 68] which, however, may be associated with a rise in temperature. The results obtained with the present data are shown in Fig. 9. T_{HeLi} is chosen as the temperature observable. The excitation energy was determined by calorimetry, as described in Refs. [24, 52], considering in particular also the neutron energies and multiplicities measured with the LAND neutron detector [69].

The obtained caloric curves exhibit the overall behavior known from earlier analyses [24] but the range of deposited energies $\langle E_0 \rangle / \langle A_0 \rangle$ covered at 1000 MeV per nucleon incident energy extends to much higher values than at 600 MeV per nucleon which is inconsistent with the universality of the spectator decay that so clearly appears in other variables [26]. Technically, the difference can be traced back to the higher kinetic energies of neutrons in the frame of the projectile spectator at small Z_{bound} and 1000 MeV per nucleon. The neutron energies measured with LAND were taken as representative also for the proton kinetic energies in this analysis. Preequilibrium nucleons from earlier reaction stages, apparently, contribute at the highest excitation energies which, therefore, have to be considered as upper limits.

Lower excitation energies, consistent with the invari-

ance of the fragment decays with respect to the incident energy, were obtained from the analysis with the Statistical Multifragmentation Model with input parameters derived from the fragment observables alone [25]. In this so-called backtracing procedure (see also Refs. [70, 71]), an ensemble of input sources with varying mass and excitation energy is chosen and adjusted to reproduce the measured fragment-charge spectra and fragment correlations. The excitation energies of these sources are used in Fig. 10. They should be considered as lower limits, however, since the fragment kinetic energies are underestimated by the model (Refs. [21, 26] and previous subsection).

The significance and interpretations of the caloric curve for chemical freeze-out, widely discussed in the literature, have very recently been summarized by Kelić et al. [49]. Analyses with statistical and dynamical models show that the plateau-like part of the caloric curve may be identified with the transition region between the liquid nuclear phase and a disordered phase of particles and fragments (see, e.g., Refs. [38, 72, 73, 74, 75, 76, 77, 78]). The methods and limitations of determining the excitation energy at the breakup stage have been reviewed by Viola and Bougault [79].

The model comparison of the Z_{bound} dependence of the measured temperature avoids the problems of calorimetry. In the backtracing analyses with the Statistical Multifragmentation Model presented in Refs. [25, 80], the observed small rise of the temperature with decreasing Z_{bound} has been quantitatively reproduced. The obtained apparent T_{HeLi} , calculated with adjusted ensembles of fragmenting sources, was found to agree well with the experimental data. It was, furthermore, found to be slightly lower than the thermodynamical model temperature, by an amount consistent with a side-feeding correction of, on average, about 20%. In more detail, the deviations turned out to be larger at the smaller excitations than at higher excitations corresponding to small values of Z_{bound} (Fig. 7 in Ref. [25] and Fig. 2 in Ref. [80]). Within this model, the predicted plateau of the breakup temperature $T \approx 6$ MeV for excitation energies between 4 and about 8 MeV is thus consistent with the observed smooth rise of the chemical temperatures of light fragments in this interval.

In these calculations, the channels with smaller Z_{bound} are populated by the decay of spectator sources of smaller mass and higher excitation, in accordance with the geometrical participant-spectator scenario. The rise of the breakup temperature with decreasing Z_{bound} , in this way, translates into a mass dependence which is found to be rather generally obeyed in multifragment decays [81]. In data from several experiments, temperatures $T \approx 6$ MeV are associated with heavy systems of mass $A \approx 200$ while higher temperatures up to $T \approx 8$ MeV are observed for lighter systems with $A < 100$. The steady rise of the temperature with excitation energy for the very small systems has even been interpreted as indicating a breakup at conditions close to the critical point [82].

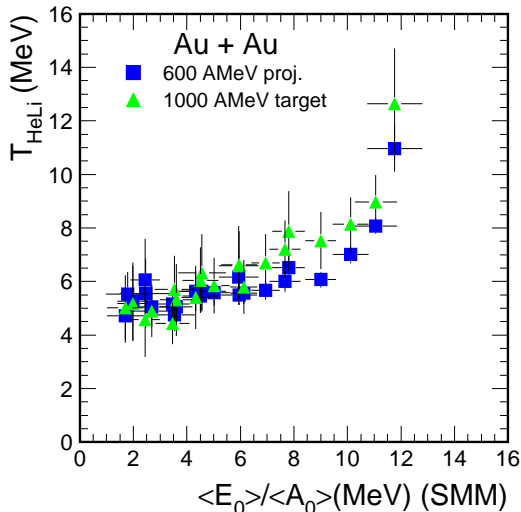


FIG. 10: (Color online) Caloric curves obtained for ^{197}Au on ^{197}Au at 600 and 1000 MeV per nucleon with temperatures T_{HeLi} and excitation energies as obtained from the statistical-model description of the fragment observables [21, 52].

This systematic dependence has been associated with the concept of the limiting temperature at which excited homogeneous systems become unbound [83]. According to these finite-temperature Hartree-Fock calculations, the limiting temperature should not only depend on the mass of the system but, because of the changing Coulomb pressure, also on its isotopic composition. This prediction, however, has so far not been confirmed experimentally. The T_{HeLi} temperatures for target spectator decays initiated by ^{12}C projectiles of 300 and 600 MeV per nucleon on ^{112}Sn and ^{124}Sn targets differ by not more than 0.5 MeV for similarly violent collisions [51], while a difference of about 1.5 MeV would be expected according to the calculations [83]. However, in accordance with the predictions, the more proton-rich ^{112}Sn system exhibits the lower temperature on average.

E. Internal excitation

The measured excited-state temperatures of 5 to 6 MeV reflecting the internal excitation of the observed He, Li and Be isotopes are in good agreement with other measurements performed with the same method and for reaction channels characterized by multiple fragment production [3, 10, 11, 84]. Higher temperatures of 7 to 9 MeV have been reported for excited ^6Li fragments in ^{14}N on ^{197}Au reactions at 35 MeV per nucleon after selecting the d- α pairs with the highest pair momenta while typical temperatures were 3 to 5 MeV also for this reaction [85]. Lower temperature values measured in compound reactions were found to be of the expected magnitude which confirms the sensitivity of the excited-state populations to the thermal characteristics of the reaction

process [30, 86, 87, 88].

The internal excitation of heavier fragments at freeze-out in reactions at intermediate energies has been studied by measuring the correlations between light particles and fragments [59, 89, 90]. For the reaction ^{124}Xe on Sn at 50 MeV per nucleon, the excitation energies of fragments over a wide range of Z have been found to saturate at $E/A \approx 3$ MeV [59, 89] while a slightly lower value of 2.5 MeV has been reported for central ^{84}Kr on ^{93}Nb at 45 MeV [90] (for a review, see Ref. [91]). The corresponding temperatures of not more than 5 MeV compare well with the present results and confirm their universal character as representing the internal excitation in fragment emissions. Translated into time scales of evaporation processes, temperatures between 4 and 6 MeV correspond rather generally to nuclear life times of the order of 50 to 200 fm/c [92, 93, 94] which cover the range of time scales deduced for fragmentation reactions [48, 95, 96, 97].

These experimental methods probe the excitation of the fragments when they are sufficiently separated from the rest of the system, so that the correlations of the decay products are not disturbed by further collisions. Similarly, the particle-unstable resonances will have to acquire their asymptotic quantum structure before they can be recognized. This is not likely to occur as long as they are connected to the nuclear medium [53, 54, 98, 99]. The typical widths of about 1 MeV define very similar time scales of the order of 200 fm/c for their formation and decay. The obtained temperatures thus refer to a late stage in the reaction process whereas the chemical temperatures may reflect properties of earlier stages at which the fragments are still in contact and their chemical compositions are still being established. In a disintegration scenario associated with cooling, an observed difference of these temperatures does not necessarily rule out that the two degrees of freedom are in equilibrium up to the time when one of them freezes out (cf. Refs. [3, 100]). On the other hand, molecular dynamics calculations consistently predict differences between the internal product temperatures and those of the surrounding environment. According to quantum molecular dynamics calculations for the ^{197}Au on ^{197}Au reaction between 60 and 150 MeV per nucleon, the relative motion of the constituents of asymptotically identified light fragments, e.g. $Z = 3$, corresponds to a nearly constant $T = 5$ MeV during most of the reaction time up to 200 fm/c [65]. The environment, at the same time, cools from about 15 MeV to temperatures much below 5 MeV. Also in classical molecular dynamics calculations, the internal temperatures evolve differently from those of the hot environment [101, 102].

These arguments may be sufficient to conclude that differences between the temperatures representing the chemical composition of the fragments and the internal excitation after their release have to be expected. The observed saturation of the latter may, in fact, represent another and rather obvious evidence for the existence of a limit up to which a nucleus can be excited [103]. In the case of surface emissions from hot residues, this limit is

evidently not yet reached by the system itself which then can act as the heat reservoir determining both, the composition and internal excitation of the fragments. When the system becomes unstable with respect to bulk disintegration at higher excitations, composite products will still have to obey this limit in order to be recognized as such entities in the final partitions.

It is, nevertheless, a rather intriguing result that internal temperatures of 5 MeV are universally observed in the fragmentation channels throughout the wide range of reactions covered by the many experiments, including, e.g., also the measurement of bremsstrahlung photons [104]. The question arises whether this would have to be directly connected to the process of fragment formation in order to exhibit this generality. The problems associated with predicting internal fragment excitations at freeze-out in an expansion scenario have been recognized early on [105] after the first data on excited-state temperatures had become available [106, 107]. Values near $T = 5$ MeV have been very consistently obtained even though remarkably different theoretical approaches were followed. The presented reasons are numerous and of different origin as, e.g., coalescence heating [108, 109] or the onset of instabilities [110].

A mechanism leading to invariant internal excitations is also constituted by the Goldhaber model [62] which has been found to provide a basis for the understanding of the fragment kinetic energies in reactions at relativistic and also intermediate energies [20, 21, 63, 111]. As an example, the clusterization mechanism proposed for the production of fragments of mass number A in peripheral collisions at intermediate energies involves a random picking of A nucleons from a cold Fermi sphere [112]. Their momenta in the center-of-mass system of the formed fragment correspond to those of an excited system. This has been tested by fitting finite-temperature Fermi distributions to the mean momentum distributions obtained with a Monte Carlo procedure following this prescription. The resulting temperatures drop, approximately like $1/\sqrt{A}$, from about 7 MeV for $A = 5$ to smaller values for larger clusters [112]. For intermediate-mass fragments, this is of the order of magnitude that is observed. More importantly, this mechanism is fairly independent of the global course of the reaction and of the excitation of the emitting system.

V. CONCLUSION AND OUTLOOK

A summary has been presented of a series of temperature measurements for spectator decays following the excitation of ^{197}Au nuclei in relativistic collisions at energies up to 1 GeV per nucleon. The methods used permit the determination of the temperature representing the assumed thermal population of the considered degrees of freedom. They are model independent except for the assessment of the effects of sequential decay which, however, are important, in particular for temperatures

derived from double isotope-yield ratios. Kinetic energies and the kinetic temperatures associated with them were only briefly addressed. Rather than collective motion, the Fermi motion of nucleons in the colliding nuclei are evidently responsible for their high values which considerably exceed the thermal and chemical breakup temperatures in the reactions studied here.

The main observation derived from the data and discussed in detail is the divergence of the isotope and excited-state temperatures with increasing excitation of the spectator system. The chemical and thermal freeze-outs cease to coincide if bulk disintegrations of major parts of the excited intermediate system start to become important, i.e., at the point of transition from residue formation to multifragment production. The higher values of temperatures derived from double-isotope ratios suggest that the chemical compositions are established prior to the thermal freeze-out stage when the products finally disconnect from the system. The thermal freeze-out temperatures deduced from excited-state populations of particle-unstable resonances saturate around $T = 5$ MeV, a value common to several classes of fragmentation reactions. In particular, the patterns observed in explosive fragmentations following central collisions of heavy systems and in the largely equilibrated spectator decays studied here are rather similar.

The chemical freeze-out temperatures have characteristic properties in common with the partitions themselves as, e.g., the invariance properties of Z_{bound} -sorted observables. Here, the invariance with respect to the mass of the collision partner and the invariance with the bombarding energy in the studied range of 600 to 1000 MeV per nucleon have been explicitly demonstrated. As a new result, it is found that the T_{BeLi} thermometer based on fragments with $Z \geq 3$ follows the results obtained with the frequently used T_{HeLi} thermometer. Also the single ratios of isotope yields exhibit the Z_{bound} dependence that is expected from the binding-energy difference in chemical equilibrium. Only the double ratios containing carbon isotopes do not consistently support the general trend to higher temperatures at smaller Z_{bound} . With the present data, it has not been possible to firmly resolve whether this is caused by nuclear-structure effects in particular combinations of isotopes or whether, more likely, it indicates some restriction in the validity of a concept of global chemical equilibrium at breakup. Heavier products, unable to survive in very hot environments, can only come from cooler regions of the system.

The uncertainty of secondary-decay corrections remains the limiting factor in the quantitative analysis. The corrections are well under control at the lower temperatures of up to about 4 MeV and, in particular, in the case of emissions from excited residue nuclei. The uncertainties increase with the temperature and approach the MeV order of magnitude once typical breakup temperatures of 6 MeV are reached or exceeded. This was illustrated by comparing several different correction methods. While it is highly desirable to improve this situation, it

has, nevertheless, been possible to establish important trends, in good agreement with results from other experiments. A remaining open problem is constituted by the somewhat unclear role of limiting temperatures which seem to influence the internal fragment excitations but not the dependence of the chemical temperatures on the

isotopic composition of the system, at least not in the predicted magnitude.

The authors would like to thank A.S. Botvina, J.B. Natowitz, W. Reisdorf, and M.B. Tsang for fruitful discussions. This work was supported by the European Community under contract ERBFMGECT950083.

-
- [1] For a review and references to earlier reviews, see D. Ardouin, *Int. J. Mod. Phys. E* **6**, 391 (1997).
- [2] W.G. Gong, W. Bauer, C.K. Gelbke, S. Pratt, *Phys. Rev. C* **43**, 781 (1991).
- [3] J. Pochodzalla *et al.*, *Phys. Rev. C* **35**, 1695 (1987).
- [4] D.J. Morrissey, W. Benenson, W.A. Friedman, *Annu. Rev. Nucl. Part. Sci.* **44**, 65 (1994).
- [5] D.H.E. Gross, *Rep. Prog. Phys.* **53**, 605 (1990); *Phys. Rep.* **279**, 119 (1997).
- [6] J.P. Bondorf, A.S. Botvina, A.S. Iljinov, I.N. Mishustin, K. Sneppen, *Phys. Rep.* **257**, 133 (1995).
- [7] A.S. Botvina and I.N. Mishustin, *Eur. Phys. J. A* **30**, 121 (2006), and in *Dynamics and Thermodynamics with Nuclear Degrees of Freedom*, ed. by Ph. Chomaz *et al.*, Springer, Berlin Heidelberg New York, 2006.
- [8] M.J. Huang *et al.*, *Phys. Rev. Lett.* **78**, 1648 (1997).
- [9] M.B. Tsang *et al.*, *Phys. Rev. C* **53**, R1057 (1996).
- [10] V. Serfling *et al.*, *Phys. Rev. Lett.* **80**, 3928 (1998).
- [11] H.F. Xi *et al.*, *Phys. Rev. C* **58**, R2636 (1998).
- [12] H. Xi *et al.*, *Phys. Lett. B* **431**, 8 (1998).
- [13] W.C. Hsi *et al.*, *Phys. Rev. Lett.* **73**, 3367 (1994).
- [14] C. Williams *et al.*, *Phys. Rev. C* **55**, R2132 (1997).
- [15] W. Reisdorf and H.G. Ritter, *Annu. Rev. Nucl. Part. Sci.* **47**, 663 (1997).
- [16] A. Le Fèvre *et al.*, *Nucl. Phys.* **A735**, 219 (2004).
- [17] W. Reisdorf *et al.*, *Phys. Lett. B* **595**, 118 (2004).
- [18] J.P. Bondorf, D. Idier, I.N. Mishustin, *Phys. Lett. B* **359**, 261 (1995).
- [19] G.J. Kunde *et al.*, *Phys. Rev. Lett.* **74**, 38 (1995).
- [20] T. Gaitanos, H.H. Wolter, C. Fuchs, *Phys. Lett. B* **478**, 79 (2000).
- [21] T. Odeh *et al.*, *Phys. Rev. Lett.* **84**, 4557 (2000).
- [22] S. P. Avdeyev *et al.*, *Nucl. Phys.* **A709**, 392 (2002).
- [23] S. Turbide *et al.*, *Phys. Rev. C* **70**, 014608 (2004).
- [24] J. Pochodzalla *et al.*, *Phys. Rev. Lett.* **75**, 1040 (1995).
- [25] Hongfei Xi *et al.*, *Z. Phys. A* **359**, 397 (1997); erratum in *Eur. Phys. J. A* **1**, 235 (1998).
- [26] A. Schüttauf *et al.*, *Nucl. Phys.* **A607**, 457 (1996).
- [27] S. Fritz *et al.*, *Phys. Lett. B* **461**, 315 (1999).
- [28] C.A. Ogilvie *et al.*, *Nucl. Phys.* **A553**, 271c (1993).
- [29] G.J. Kunde *et al.*, *Phys. Lett. B* **272**, 202 (1991).
- [30] C. Schwarz *et al.*, *Phys. Rev. C* **48**, 676 (1993).
- [31] V. Serfling, Ph.D. thesis, Universität Frankfurt, 1997.
- [32] S. Fritz, Ph.D. thesis, Universität Frankfurt, 1997.
- [33] J. Pochodzalla and W. Trautmann, in *Isospin Physics in Heavy-Ion Collisions at Intermediate Energies*, ed. by B.-A. Li and W.U. Schröder, Nova Science, New York, 2001, p. 451.
- [34] S. Albergo, S. Costa, E. Costanzo, A. Rubbino, *Il Nuovo Cimento* **89A**, 1 (1985).
- [35] M.B. Tsang, W.G. Lynch, H. Xi, W.A. Friedman, *Phys. Rev. Lett.* **78**, 3836 (1997).
- [36] D. Hahn and H. Stöcker, *Nucl. Phys.* **A476**, 718 (1988).
- [37] J. Konopka, H. Graf, H. Stöcker, W. Greiner, *Phys. Rev. C* **50**, 2085 (1994).
- [38] S. Das Gupta and A.Z. Mekjian, *Phys. Rev. C* **57**, 1361 (1998).
- [39] J. Hubele *et al.*, *Z. Phys. A* **340**, 263 (1991).
- [40] P. Kreuz *et al.*, *Nucl. Phys.* **A556**, 672 (1993).
- [41] J.A. Hauger *et al.*, *Phys. Rev. C* **57**, 764 (1998).
- [42] Z. Majka, P. Staszal, J. Cibor, J.B. Natowitz, K. Hagel, J. Li, N. Mdeiwayeh, R. Wada, Y. Zhao, *Phys. Rev. C* **55**, 2991 (1997).
- [43] S.K. Samaddar, J.N. De, S. Shlomo, *Phys. Rev. Lett.* **79**, 4962 (1997).
- [44] R.P. Scharenberg *et al.*, *Phys. Rev. C* **64**, 054602 (2001).
- [45] Z. Chen and C. K. Gelbke, *Phys. Rev. C* **38**, 2630 (1988).
- [46] F. Gulminelli and D. Durand, *Nucl. Phys.* **A615**, 117 (1997).
- [47] H. Xi, W.G. Lynch, M.B. Tsang, W.A. Friedman, D. Durand, *Phys. Rev. C* **59**, 1567 (1999).
- [48] V.E. Viola, K. Kwiatkowski, W.A. Friedman, *Phys. Rev. C* **59**, 2660 (1999).
- [49] A. Kelić, J.B. Natowitz, K.-H. Schmidt, *Eur. Phys. J. A* **30**, 203 (2006), and in *Dynamics and Thermodynamics with Nuclear Degrees of Freedom*, ed. by Ph. Chomaz *et al.*, Springer, Berlin Heidelberg New York, 2006.
- [50] R.J. Charity *et al.*, *Nucl. Phys.* **A483**, 371 (1988).
- [51] A. Le Fèvre *et al.*, *Phys. Rev. Lett.* **94**, 162701 (2005).
- [52] T. Odeh, Ph.D. thesis, Universität Frankfurt, 1999.
- [53] A. Ono, P. Danielewicz, W.A. Friedman, W.G. Lynch, M.B. Tsang, *Phys. Rev. C* **70**, 041604(R) (2004).
- [54] A.S. Botvina, N. Buyukcizmeci, M. Erdogan, J. Lukasik, I.N. Mishustin, R. Ogul, W. Trautmann, *Phys. Rev. C* **74**, 044609 (2006).
- [55] M. Colonna and M.B. Tsang, *Eur. Phys. J. A* **30**, 165 (2006), and in *Dynamics and Thermodynamics with Nuclear Degrees of Freedom*, ed. by Ph. Chomaz *et al.*, Springer, Berlin Heidelberg New York, 2006.
- [56] D.V. Shetty, S.J. Yennello, G.A. Souliotis, *Phys. Rev. C* **75**, 034602 (2007).
- [57] B. Zwiegliński *et al.*, *Nucl. Phys.* **A681**, 275c (2001).
- [58] B. Zwiegliński *et al.*, *Acta Phys. Pol.* **B33**, 141 (2002).
- [59] S. Hudan *et al.*, *Phys. Rev. C* **67**, 064613 (2003).
- [60] J. Lauret *et al.*, *Phys. Rev. C* **57**, R1051 (1998).
- [61] L. Beaulieu *et al.*, *Phys. Rev. Lett.* **84**, 5971 (2000).
- [62] A.S. Goldhaber, *Phys. Lett.* **53B**, 306 (1974).
- [63] W. Bauer, *Phys. Rev. C* **51**, 803 (1995).
- [64] P.B. Gossiaux and J. Aichelin, *Phys. Rev. C* **56**, 2109 (1997).
- [65] K. Zbiri *et al.*, *Phys. Rev. C* **75**, 034612 (2007).
- [66] T.X. Liu *et al.*, *Europhys. Lett.* **74**, 806 (2006).
- [67] C.A. Ogilvie *et al.*, *Phys. Rev. Lett.* **67**, 1214 (1991).
- [68] B. Tamain, *Eur. Phys. J. A* **30**, 71 (2006), and in *Dynamics and Thermodynamics with Nuclear Degrees of*

- Freedom*, ed. by Ph. Chomaz et al., Springer, Berlin Heidelberg New York, 2006.
- [69] Th. Blaich et al., Nucl. Instr. Methods Phys. Res. **A314**, 136 (1992).
- [70] A.S. Botvina *et al.*, Nucl. Phys. **A584**, 737 (1995).
- [71] P. Désesquelles, J.P. Bondorf, I.N. Mishustin, A.S. Botvina, Nucl. Phys. **A604**, 183 (1996).
- [72] J.N. De, S. Das Gupta, S. Shlomo, S.K. Samaddar, Phys. Rev. C **55**, R1641 (1997).
- [73] S.J. Lee and A.Z. Mekjian, Phys. Rev. C **56**, 2621 (1997).
- [74] J. Schnack and H. Feldmeier, Phys. Lett. B **409**, 6 (1997).
- [75] Y. Sugawa and H. Horiuchi, Phys. Rev. C **60**, 064607 (1999).
- [76] A. Le Fèvre, O. Schapiro, A. Chbihi, Nucl. Phys. **A657**, 446 (1999).
- [77] Al.H. Raduta and Ad.R. Raduta, Phys. Rev. C **61**, 034611 (2000).
- [78] T. Furuta and A. Ono, Phys. Rev. C **74**, 014612 (2006).
- [79] V.E. Viola and R. Bougault, Eur. Phys. J. A **30**, 215 (2006), and in *Dynamics and Thermodynamics with Nuclear Degrees of Freedom*, ed. by Ph. Chomaz et al., Springer, Berlin Heidelberg New York, 2006.
- [80] J.P. Bondorf, A.S. Botvina, I.N. Mishustin, Phys. Rev. C **58**, R27 (1998).
- [81] J.B. Natowitz, R. Wada, K. Hagel, T. Keutgen, M. Murray, A. Makeev, L. Qin, P. Smith, C. Hamilton, Phys. Rev. C **65**, 034618 (2002).
- [82] Y.G. Ma *et al.*, Phys. Rev. C **69**, 031604(R) (2004).
- [83] J. Besprosvany and S. Levit, Phys. Lett. B **217**, 1 (1989).
- [84] F. Zhu, *et al.*, Phys. Rev. C **52**, 784 (1995).
- [85] C.B. Chitwood, C.K. Gelbke, J. Pochodzalla, Z. Chen, D.J. Fields, W.G. Lynch, R. Morse, M.B. Tsang, D.H. Boal, J.C. Shillcock, Phys. Lett. B **172**, 27 (1986).
- [86] T.K. Nayak *et al.*, Phys. Rev. Lett. **62**, 1021 (1989); Phys. Rev. C **45**, 132 (1992).
- [87] H. Dabrowski *et al.*, Phys. Lett. B **247**, 223 (1990).
- [88] F. Zhu *et al.*, Phys. Lett. B **322**, 43 (1994).
- [89] N. Marie *et al.*, Phys. Rev. C **58**, 256 (1998).
- [90] P. Staszal *et al.*, Phys. Rev. C **63**, 064610 (2001).
- [91] G. Verde, A. Chbihi, R. Ghetti, J. Helgesson, Eur. Phys. J. A **30**, 81 (2006), and in *Dynamics and Thermodynamics with Nuclear Degrees of Freedom*, ed. by Ph. Chomaz et al., Springer, Berlin Heidelberg New York, 2006.
- [92] W.A. Friedman and W.G. Lynch, Phys. Rev. C **28**, 16 (1983).
- [93] B. Borderie, Ann. Phys. Fr. **17**, 349 (1992).
- [94] J. Navarro, P.-G. Reinhard, E. Suraud, Eur. Phys. J. A **30**, 333 (2006), and in *Dynamics and Thermodynamics with Nuclear Degrees of Freedom*, ed. by Ph. Chomaz et al., Springer, Berlin Heidelberg New York, 2006.
- [95] C. Schwarz *et al.*, Nucl. Phys. **A681**, 279c (2001).
- [96] V.K. Rodionov *et al.*, Nucl. Phys. **A700**, 457 (2002).
- [97] V.E. Viola *et al.*, Phys. Rep. **434**, 1 (2006).
- [98] P. Danielewicz and Q. Pan, Phys. Rev. C **46**, 2002 (1992).
- [99] T. Alm, G. Röpke, A. Schnell, H. Stein, Phys. Lett. B **346**, 233 (1995).
- [100] Z. Chen *et al.*, Phys. Rev. C **36**, 2297 (1987).
- [101] H.W. Barz, J.P. Bondorf, D. Idier, I.N. Mishustin, Phys. Lett. B **382**, 343 (1996).
- [102] X. Campi, H. Krivine, E. Plagnol, N. Sator, Phys. Rev. C **67**, 044610 (2003).
- [103] S.E. Koonin and J. Randrup, Nucl. Phys. **A474**, 173 (1987).
- [104] D.G. d'Enterria *et al.*, Phys. Rev. Lett. **87**, 022701 (2001).
- [105] D.H. Boal, J.N. Glosli, C. Wicentowich, Phys. Rev. C **40**, 601 (1989).
- [106] D.J. Morrissey, W. Benenson, E. Kashy, B. Sherrill, A.D. Panagiotou, R.A. Blue, R.M. Ronningen, J. van der Plicht, H. Utsunomiya, Phys. Lett. **148B**, 423 (1984).
- [107] J. Pochodzalla *et al.*, Phys. Rev. Lett. **55**, 177 (1985).
- [108] W.A. Friedman, Phys. Rev. Lett. **60**, 2125 (1988).
- [109] H.-W. Barz, J.P. Bondorf, R. Donangelo, H. Schulz, K. Sneppen, Phys. Lett. B **228**, 453 (1989).
- [110] C. Fuchs, P. Essler, T. Gaitanos, H.H. Wolter, Nucl. Phys. **A626**, 987 (1997).
- [111] J. Lukasik *et al.*, Phys. Rev. C **66**, 064606 (2002).
- [112] J. Lukasik *et al.*, Phys. Lett. B **566**, 76 (2003).